IEEE Access
Multidisciplinary | Rapid Review | Open Access Journal

Received June 16, 2020, accepted July 4, 2020, date of publication July 9, 2020, date of current version July 22, 2020.

Digital Object Identifier 10.1109/ACCESS.2020.3008181

Solar-CTP: An Enhanced CTP for Solar-Powered Wireless Sensor Networks

SEOK HYUN CHEONG[1], MINJAE KANG[2], YOUNGHYUN KIM[3], (Member, IEEE), MINHO PARK[4], (Member, IEEE), JINHO PARK[5], AND DONG KUN NOH[1], (Member, IEEE)

[1]Department of Software Convergence, Soongsil University, Seoul 06978, South Korea
[2]Department of Electronic Engineering, Soongsil University, Seoul 06978, South Korea
[3]Department of Electrical and Computer Engineering, University of Wisconsin–Madison, Madison, WI 53706, USA
[4]School of Electronic Engineering, Soongsil University, Seoul 06978, South Korea
[5]Global School of Media, Soongsil University, Seoul 06978, South Korea

Corresponding author: Dong Kun Noh (dnoh@ssu.ac.kr)

This work was supported by the Soongsil University Research Fund (Convergence Research) of 2019.

ABSTRACT Wireless sensor networks (WSNs) suffer not only from short lifetimes because of limited energy but also from an energy imbalance between the nodes close to the sink and the other nodes. To fundamentally resolve the issue of short lifetimes, recent studies have utilized environmental energy, such as solar power. Additionally, WSNs that employ energy-aware dynamic topology control are also being studied to address the energy imbalance. This paper proposes an improved collection tree protocol (CTP) scheme, called solar-CTP, that uses the two approaches of energy-harvesting and energy-aware topology control simultaneously. The proposed scheme is derived from the CTP scheme, which is a widely adopted data collection strategy designed for typical battery-based WSNs with a fixed sink. We tailor the CTP scheme for solar-powered WSNs operating with a mobile sink. Performance verification confirms that our scheme significantly reduces the number of blackout nodes compared to other CTP variants, thus increasing the amount of data collected by the sink.

INDEX TERMS Wireless sensor network, solar-powered, mobile sink, CTP, solar-CTP.

I. INTRODUCTION

A wireless sensor network (WSN) refers to a group of spatially dispersed sensors for monitoring the physical conditions of the environment and gathering sensory data at a central location called the sink node. WSNs are widely used in various fields, such as disaster monitoring, environmental sensing, health care monitoring, and threat detection [1], [2]. Sensor nodes are produced at low cost and distributed in small sizes but in large quantities. They therefore face the issue of short lifetime due to battery resource constraints. To solve this problem, research on energy-harvesting sensors that continuously collect energy from the surrounding environment is actively being conducted [3]. In particular, solar energy is the most suitable form of environmental energy for sensor nodes because of its high energy density and periodicity. Meanwhile, because of the fixed position of the sink node, the nodes closer to the sink node experience more energy consumption than the farther nodes, leading to the problem of energy imbalance [4]. This energy imbalance can be reduced to some extent by using a mobile sink node that periodically shifts its position to gather sensory data [5]. In this study, we address both the problems of short lifetimes and an energy imbalance simultaneously.

The collection tree protocol (CTP) [6] is a widely used routing scheme for effectively collecting data in WSNs. This scheme was originally designed for WSNs consisting of battery-based sensor nodes and a fixed sink node. It performs routing by constructing a tree topology based on the expected transmission number (ETX) [7], which is an indicator of the link quality. The CTP has the advantages of high data throughput and hardware independence but also has the drawbacks of severe energy imbalance between nodes and the possibility of loop occurrence. Relatively high energy consumption can occur not only at the higher levels of the tree (i.e., the nodes near the sink node) but also in any parent nodes communicating with many child nodes. This energy imbalance eventually leads to short lifetimes of the entire network. To address these problems, we propose the solar-CTP protocol, which tailors and improves the CTP for

The associate editor coordinating the review of this manuscript and approving it for publication was Maurice J. Khabbaz.

solar-powered WSNs operating with a mobile sink. The problems and solutions in this scheme are summarized in Fig. 1 and described below:

1) **Energy constraints:** Addressed by adopting solar energy-harvesting and overcoming limitations of solar-unaware CTP routing.
2) **Blackout nodes:** Addressed by using an energy-aware scheme for determining the operation mode and parent selection that considers not only the link quality but also the energy budget.
3) **Energy imbalance:** Addressed by adaptively reconstructing the tree topology according to the energy status, link quality, and location of the mobile sink node.

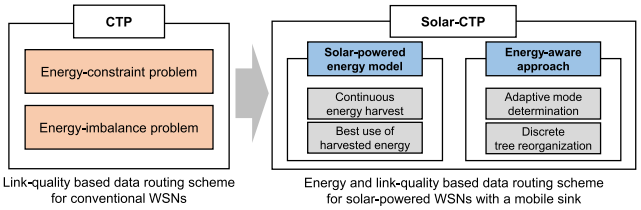

FIGURE 1. Contributions of solar-CTP.

Note that even with a solar-based sensor node, blackouts can still occur at certain periods of time when more energy is consumed than harvested on average. On the other hand, if the focus is placed only on saving energy as in a battery-based sensor node, the residual energy in the rechargeable battery will gradually increase, and the surplus energy will have to be discarded when the capacity limit of the rechargeable battery is reached. Therefore, we designed our solar-CTP to utilize the harvested solar energy efficiently, yet without discarding excessive energy [8].

This paper is organized as follows. In Section II, we review previous research concerning both solar-powered WSNs and CTP. In Section III, we introduce our scheme in detail, which represents an enhanced CTP for solar-powered WSNs operating with a mobile sink. Section IV verifies the performance of our scheme by comparing it with the performances of other schemes, and we present our conclusions in Section V.

II. RELATED WORK

A. ENERGY-HARVESTING WSNs

Conventional WSNs suffer from short lifetimes due to battery resource constraints. To solve this problem, many studies have been conducted to minimize the node energy consumption [9]–[14]. However, minimizing energy consumption alone cannot be the fundamental solution to the limited lifetime. Additional maintenance costs, such as manual battery replacements, are incurred for conventional WSNs to operate continuously. To solve this problem, studies have been performed on energy-harvesting wireless sensor nodes capable of continuously harvesting environmental energy. Table 1 [15] shows a comparison of various energy sources and their power densities.

TABLE 1. Energy-harvesting sources and power densities.

Energy source	Power density
Solar	15 mW/cm^2
RF	0.1 μW/cm^2
Wind	16.2 μW/cm^3
Acoustic noise	960 nW/cm^3
Motion	330 μW/cm^3
Body heat	40 μW/cm^2

Because solar energy can be harvested periodically and has a high power density compared to other sources, it can satisfy the energy requirements for operating sensor nodes. Therefore, unlike battery-based WSNs, which aim to minimize energy consumption, research on solar-powered wireless sensor nodes has focused on the prediction and efficient use of harvested energy. As mentioned before, solar-powered nodes should keep the average energy consumption from exceeding the harvested energy but, at the same time, should not waste energy due to limited energy storage. Therefore, a scheme for predicting and scheduling energy income and outcome is crucial for solar-powered nodes.

Kansal *et al.* [16] proposed an energy model for solar-powered nodes and an algorithm for determining the energy that enables a node to operate permanently. Moser *et al.* [17] predicted the amount of harvested energy using the moving average model. Piorno *et al.* [18] proposed a method of predicting the amount of harvested energy based on forecasted weather conditions. Cammarano *et al.* [19] proposed a more accurate prediction method through short- and long-term forecasts based on the weather and season. Noh and Kang [20] and Zhang *et al.* [21] proposed balanced energy allocation methods for steadily using solar energy regardless of the time to overcome the large variation in the harvested energy at different times of the day. Yang *et al.* [22] improved the data reliability by using surplus energy through an energy threshold model based on the energy-harvesting and consumption rates. Kang *et al.* [23] proposed a method to support an efficient location service for a mobile sink by utilizing the surplus energy of solar-powered WSNs. Herrería-Alonso *et al.* [24] proposed a novel energy prediction model that makes use of the altitude angle of the sun at different times of day to predict future solar energy availability.

In addition, research on supplying energy to nodes using wireless power transmission is also actively underway. Wang *et al.* [25] proposed a hybrid framework to overcome the constraints of wireless charging and environmental harvesting techniques. In this hybrid framework, cluster heads are equipped with solar panels to scavenge solar energy, and the rest of the nodes are powered by wireless charging. First, the authors studied how to minimize the total cost of deploying a set of sensor nodes. Second, they examined the energy balance in the network and developed a distributed head reselection algorithm to designate some wireless-powered

nodes as cluster heads when solar energy is not available during rainy or cloudy days. Third, they focus on how to optimize the joint tour consisting of both wireless charging and data gathering sites for the mobile chargers. Recently, Angurala *et al.* [26] proposed a new AODV routing protocol that is modified for a wireless-recharging sensor network. In this scheme, to maintain the required energy level of the nodes, the mobile charger called SenCar visits the chosen anchor point along the predefined trajectory. At the chosen point, SenCar tests all the nodes within its coverage and re-energizes all the nodes that have an energy level below the threshold value. Then, the SenCar moves on to the next anchor point and so on until the predefined trajectory completes.

B. CTP OVERVIEW

The CTP is a protocol that performs data routing by constructing a topology based on the link quality [27], similar to DSDV [28], AODV [29], MultihopLQI [30], and RPL [31]. Note that the CTP uses ETX (expected transmission number) as the link quality indicator. Therefore, the tree structure is determined according to the ETX value of each node. The CTP has already been implemented as one of the protocol stacks of TinyOS [32] and is widely used in WSNs. The CTP does not need the address information of neighboring nodes or additional hardware to perform routing and has an excellent data transfer rate.

The CTP is composed of three modules to achieve efficient routing, as shown in Fig. 2. We briefly describe these modules and how the ETX value is managed and updated.

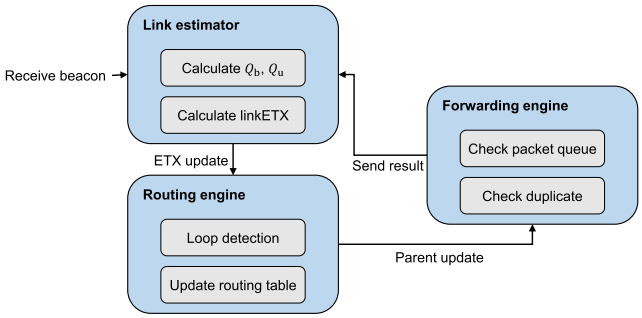

FIGURE 2. CTP module diagram.

1) **Link estimator**: The link estimator estimates the linkETX of neighboring nodes within a hop where linkETX is the expected number of transmissions that should be performed when communicating with the neighboring nodes. It can be estimated using broadcast beacons or through direct communication between nodes.
The first linkETX estimation Q_b is based on the broadcast beacon messages received from neighboring nodes and can be calculated as

$$Q_b = \frac{n_b}{N_b}, \tag{1}$$

where n_b is the number of beacons successfully received, and N_b is the number of all the beacons sent by the neighboring nodes [33]. Q_b is mainly used when the CTP is initially configured and when network imbalance issues such as loop detection occur.
The second linkETX estimation Q_u is based on direct communication with a parent node and can be calculated as

$$Q_u = \frac{n_u}{n_a}, \tag{2}$$

where n_u is the total number of packets sent by child nodes, and n_a is the number of successfully received ACK packets [33]. Q_u is used in normal topology and is a more accurate estimation method than Q_b. The linkETX estimated using these two methods is delivered to the routing engine.
2) **Routing engine**: The routing engine constructs the routing table based on the linkETX estimated by the link estimator. The ID of neighboring nodes, the linkETX with neighboring nodes, and the ETX of neighboring nodes are recorded in this routing table. The routing engine selects the node with the smallest sum of the linkETX and ETX among the neighbors as the parent node. Then, its own ETX is updated to this smallest sum. The routing engine plays a key role in finding the best routing path to the sink that has the smallest total number of expected transmissions.
3) **Forwarding engine**: The forwarding engine is responsible for the following three tasks. First, it transmits data to the parent node by checking the transmission queue. Second, it checks for packet duplication. Last, it helps to estimate the linkETX of the parent node by informing the link estimator of the data transmission results.

The CTP achieves fair data transfer rates by implementing the three modules described above using the 4-bit link-status estimator [34] and the Trickle beacon period control scheme [35]. However, the CTP also has several disadvantages. The data transfer rate of CTP is reduced when the links change suddenly. Furthermore, the CTP is vulnerable to energy imbalance, as it considers the link quality but does not consider the energy status of nodes at all. Thus, blackouts in nodes can easily occur and cause fatal problems that accelerate energy consumption across the network.

C. CTP VARIANTS

To address the aforementioned limitations of the CTP, much research has been conducted recently. Table 2 shows a summary of the contributions of the schemes that address the problems of the CTP, followed by a brief description of each scheme [36]–[41].

1) BCTP [36] determines whether a node is a hotspot based on the number of transmissions measured over a specific period. When the node is determined to be a hotspot, its child nodes find new parent nodes.

TABLE 2. Contribution of various CTP schemes.

Scheme \ Contribution	Load balancing	Link dynamics	Loop avoidance
BCTP	⋁		⋁
O-CTP		⋁	
RCTP		⋁	⋁
E-CTP	⋁		
La-CTP			⋁
DP-CTP		⋁	

This scheme solves the traffic imbalance of some nodes by determining the hotspots and changing the parents. However, it has poor performance in environments where the link quality is not good because it considers only the number of transmissions. Additionally, energy imbalance can still occur because it does not consider the energy consumption of the nodes.

2) O-CTP [37] is designed to respond to sudden link changes. In this scheme, when the link quality is degraded, the node that detects the degradation probabilistically broadcasts to all its neighboring nodes heading towards the sink node. This leads to a higher data transfer rate than that of the CTP when the link quality is poor, but the nodes located near the sink unnecessarily consume more energy by receiving many duplicate packets.
3) ETX has the limitation that the routing path of nodes may not be an appropriate indicator because it does not immediately reflect sudden link changes. To address this limitation, RCTP [38] was proposed to use AETX, which is the average of the three most recently measured ETXs, to achieve a higher data transfer rate. It also presented two methods to suppress loop occurrence: 1) a scheme that gives color codes to nodes based on their distance from the sink node and 2) a scheme that records the seven nodes that have recently sent data to each node so that the node does not select them as its parent node. However, this scheme also does not consider the energy consumption of the nodes and can cause energy imbalances similar to those in BCTP [36].
4) E-CTP [39] considers the energy imbalance problem where energy consumption varies depending on the position of the deployed nodes. Because the voltage of the battery can be used to identify the amount of residual energy, E-CTP compares the supply voltage of the nodes with a certain threshold voltage. The threshold voltage is defined by

$$V_T = \frac{V_{\max} + V_L}{2}, \tag{3}$$

where $V_{\max}$ is the maximum supply voltage and V_L is the voltage that the data collected would be meaningless, although the node is still able to collect information. When the supply voltage of a specific node is lower than the threshold voltage, it is considered to have a small amount of energy. Therefore, E-CTP tries to resolve this energy imbalance by reducing the probability of this node being selected as a parent node by increasing its ETX. However, there is a drawback that a child node cannot quickly notice that the ETX of its parent node has increased. This may lead to a routing loop, which delays the time that data arrive at the sink and accelerates energy consumption in the neighboring nodes.
5) La-CTP [40] is a variant of CTP focusing on suppressing and removing routing loops. Noting that the condition for changing parents in the original CTP scheme causes frequent changes in the network topology and the occurrence of routing loops, La-CTP suggested new parent change conditions to suppress loop occurrences. However, loops are not reduced completely, and the loops once generated are not removed. To remove routing loops, a new beacon transmission period control scheme was suggested. This scheme solves the loop problem by initializing the beacon transmission period of the nodes that do not receive data for a certain duration. This scheme showed a better performance than the conventional CTP in experiments conducted in various environments. Again, however, the scheme has the drawback that energy imbalance can occur because it focuses only on loop suppression and resolution.
6) DP-CTP [41] is designed for mobile WSNs. Most existing CTPs experience frequent link breaks in mobile WSNs, which cause continuous topology reconfiguration. DP-CTP presented a directional ETX that reflects the current moving direction of nodes on ETX. Through this, each node selects one of the neighbors moving in the same direction as the parent node, thereby reducing the number of topology reconstructions and increasing the amount of data gathered at a sink node.

III. PROPOSED SCHEME

A. SOLAR-CTP OVERVIEW

This section describes the proposed solar-CTP that is tailored for WSNs consisting of a mobile sink node and solar energy-harvesting nodes. Each node in this scheme determines its operation mode according to its energy status estimated based on the expected rates of energy harvest and consumption [20]. At the start of each time slot, the node compares the amount of (preallocated) energy it can use during this time slot with the amount of energy it expects to consume during this time slot. We use the expression that the energy is sufficient or enough when the former is larger, and the energy is insufficient in the opposite case. Each node operates in one of the following three modes during the time slot depending on its energy status:

1) **Normal mode**: If a node has enough energy, it performs sensing and data transfer normally.
2) **Switch mode**: When the energy is insufficient, it starts to operate in switch mode and tries to detach some of its child nodes to reduce energy consumption and prevent blackout, so that switch back to the normal mode.
3) **Control mode**: If the node cannot find any appropriate child nodes to detach in switch mode, this means that the blackout cannot be prevented by only changing the topology. Then, the node goes into the control mode with the changed topology in switch mode and tries to further minimize its blackout by decreasing the total amount of transferred data.

Fig. 3 illustrates the overall operation of the proposed scheme, including the mode changes. Whether there is enough available energy for the time slot is determined at the beginning of each time slot. Assume that node n_3 has been operating in normal mode in the previous time slot, but it predicts an energy shortage for the next time slot; thus, it enters the switch mode. As shown in Fig. 3(a), it first broadcasts a switch message to ask its child nodes (nodes n_6, n_8, and n_9) to check if their parent can be changed. Among the child nodes that send a positive reply, it chooses the most appropriate set of nodes. The nodes in this set can allow the current parent node (node n_3) to operate in normal mode if they are adopted by new parents. Node n_6 is the only member of this set in the figure. Then, node n_3 sends a change message to all the selected child nodes (node n_6 in this figure) to change their parents. As a result, node n_3 can continue to operate in normal mode. On the other hand, Fig. 3(b) shows the case where node n_3 cannot find any appropriate set of child nodes while in switch mode. All of its child nodes have sent back negative reply messages to node n_3. Therefore, node n_3 goes into the control mode and tries to prevent its blackout by decreasing the total amount of transferred data.

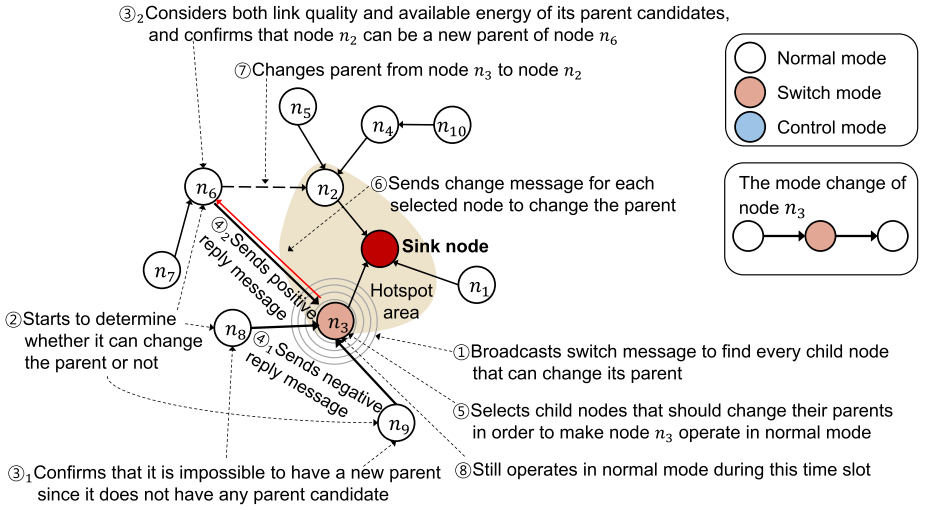

(a) A situation where node n_3 can operate still in normal mode during the next time slot

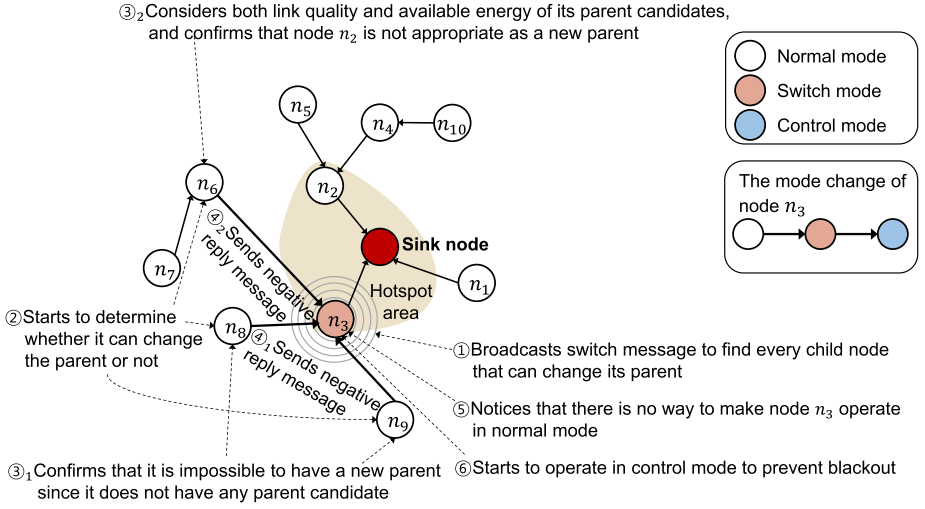

(b) A situation where node n_3 should operate in control mode during the next time slot

FIGURE 3. Overview of solar-CTP.

From now on, we would use the symbols defined in Table 3 to explain our solar-CTP in more detail.

TABLE 3. List of notations.

Notation	Description
ETX_i	ETX of node i
ETX_{parent}	ETX of the parent node
$linkETX_{(i,parent)}$	LinkETX between node i and its parent node
$E^{\text{alloc}}_{\text{remain}}(i,t+1)$	Expected amount of allocated energy of node i
$E_{\text{alloc}}(i,t)$	Allocated energy to node i
$E_{\text{sys}}(i,t)$	All the energy consumed by node i other than transmission
$E_{\text{tx}}(i,t)$	Energy consumed by node i for each data transmission
S	Size of the data to be sent
β	Energy consumed per byte during transmission
d	Distance between node i and its parent node
α	Path loss rate
$ETX_{newParent}$	ETX of the new parent node
$ETX_{originParent}$	ETX of the original parent node
$\min(linkETX_{(j,child)})$	Minimum value of the linkETX between node j and its child nodes
γ_i	Transmission control rate of node i
$S^{\max}_{\text{tx}}(i,t)$	Maximum data size that node i can transmit
$S_{\text{all}}(i,t)$	Sum of expected amount of sensing data and data from all child nodes of node i

B. INITIAL CTP CONFIGURATION

At the network startup stage, a node calculates the ETX of its neighboring nodes and updates its own ETX by receiving broadcast beacon messages, as shown in Fig. 4. The ETX of node i is defined by

$$ETX_i = ETX_{parent} + linkETX_{(i,parent)}, \tag{4}$$

where ETX_{parent} is the ETX of the parent, and $linkETX_{(i,parent)}$ is the linkETX between the parent node and node i measured by the link estimator described in Section II-B. Because the ETX of each node can be obtained from its parent's ETX, the ETX is sequentially updated from the top to the bottom of the tree. Note that node i calculates ETX_i between itself and every neighbor and then selects the node with the smallest ETX as its parent node. The value is set as the final ETX of node i (ETX_i). Then, node i continues to configure the CTP by broadcasting a beacon message containing its ETX to its neighbors.

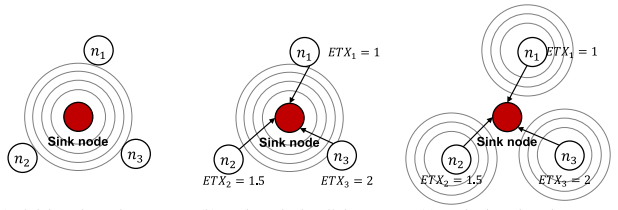

(a) Sink broadcasts beacon (b) Nodes calculate linkETX (c) Nodes broadcast beacon

FIGURE 4. CTP initial configuration by beacon message.

C. ENERGY MODEL

Fig. 5 shows that the harvested solar energy varies significantly over time depending on the availability of the sun and the weather conditions. In particular, there is little energy harvested after sunset, which is likely to cause node blackout. Additionally, surplus energy in excess of the battery capacity, which cannot be stored, may occur due to intensive energy collection during the daytime. Thus, an energy allocation scheme that determines the available energy to consume during a time slot to achieve uniform operation independent of time is necessary. We divided a day into N slots, and sensor nodes allocate available energy to each slot by using the balanced energy allocation scheme proposed by Noh and Kang [20]. Fig. 5 depicts the balanced energy allocation over N time slots.

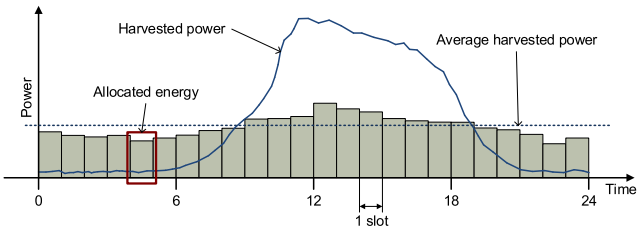

FIGURE 5. Energy allocation to the time slots.

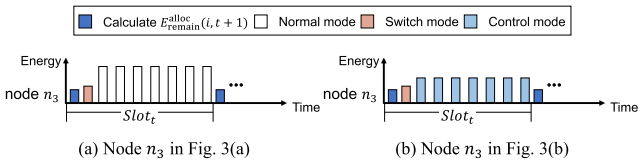

(a) Node n_3 in Fig. 3(a) (b) Node n_3 in Fig. 3(b)

FIGURE 6. Change of node operation mode over time.

As shown in Fig. 6, node i calculates the expected amount of allocated energy $E^{\text{alloc}}_{\text{remain}}(i,t+1)$ at the beginning of time slot t based on the expected energy consumption and collection during the next time slot:

$$E^{\text{alloc}}_{\text{remain}}(i,t+1) = E_{\text{alloc}}(i,t) - E_{\text{sys}}(i,t) - linkETX_{(i,parent)}E_{\text{tx}}(i,t), \tag{5}$$

where $E_{\text{alloc}}(i,t)$ is the allocated energy to node i, $E_{\text{sys}}(i,t)$ refers to all the energy consumed for purposes other than transmission, $linkETX_{(i,parent)}$ is the linkETX between node i and the parent of node i, and $E_{\text{tx}}(i,t)$ is the energy consumed by node i for each data transmission to the parent node [42]:

$$E_{\text{tx}}(i,t) = S\beta d^{\alpha}, \tag{6}$$

where S is the size of the data to be sent, β is the energy consumed per byte during transmission, d is the distance between node i and its parent node, and α is the path loss rate. Note that (6) alone is the energy consumption for data transmission in an environment where successful transmission is ensured with only one transmission. However, in reality, frequent retransmission occurs due to various interference sources present in WSNs. Therefore, the data transmission energy consumption considering the link quality is more accurately calculated by considering the ETX value, $linkETX_{(i,parent)}$.

D. NODE OPERATION MODE DETERMINATION

Algorithm 1 describes the pseudocode of the mode determination algorithm of node i. This algorithm is invoked at the start of each time slot. First, node i obtains the amount of allocated energy for time slot t (line 3 of Algorithm 1). Then, it calculates the value of $E^{\text{alloc}}_{\text{remain}}(i, t+1)$ using (5) (line 5 of Algorithm 1). Finally, depending on the calculated value of $E^{\text{alloc}}_{\text{remain}}(i, t+1)$, the operation mode of node i is determined (from line 7 to the end in Algorithm 1). If it is expected that node i can satisfy

$$E^{\text{alloc}}_{\text{remain}}(i, t+1) > 0 \tag{7}$$

Algorithm 1 Determination of the Operation Mode

```
1:  //This algorithm is invoked at every start of time slot;
2:
3:  E_alloc(i,t) = getAllocEnergy(slot_t);
4:
5:  E^alloc_remain(i,t+1) =
    E_alloc(i,t) − E_sys(i,t) − linkETX_(i,parent) S_all(i,t) β d^α;
6:
7:  if E^alloc_remain(i,t+1) > 0 then
8:      ChangeMode(Normal);
9:  else
10:     ChangeMode(Switch);
11:     Do Algorithm 2; // invokes switch mode function
```

at the end of time slot t (i.e., at the beginning of time slot $t+1$), it operates in normal mode with current topology because the expected energy consumption is less than the allocated energy. If not, it means that the expected energy consumption would be more than the allocated energy during this time slot t. Therefore, the node goes to the switch mode and tries to detach some of its child nodes to avoid blackout. If the blackout of the node can be prevented by changing the topology in this switch mode, the node returns to normal mode from the switch mode while maintaining the changed topology. However, if blackout cannot be prevented even after removing all possible child nodes in switch mode, it goes to the control mode to further reduce blackout by decreasing the amount of data sent. Of course, nonetheless, our scheme cannot rule out the possibility of blackout but tries to minimize the blackout.

Fig. 7 shows the flow chart of the node's operation modes in solar-CTP. If the node has enough energy, it goes to the normal mode. If not, it goes to switch mode and tries to change the topology according to the energy status, and then it finally determines its operation mode for this time slot between normal mode and control mode. Once the normal mode and control mode have been determined, no other mode is taken during that time slot.

E. SWITCH MODE OPERATION

If node i determines that it cannot satisfy (7) for a time slot, some of its child nodes should be detached to prevent

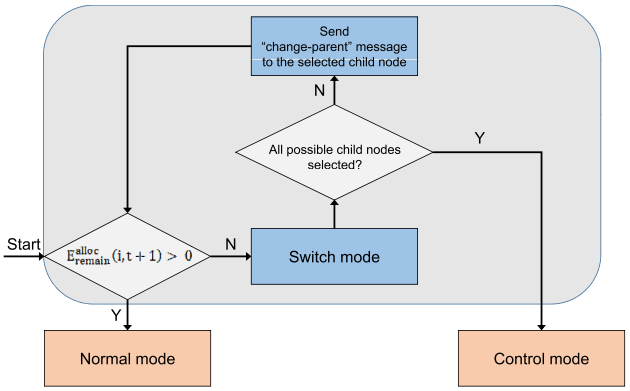

FIGURE 7. Flow chart of the node's mode change.

blackout. In this work, the node broadcasts a switch message to all of its child nodes to find which of them can be adopted by a new parent. When node j receives a switch message broadcasted from its parent node, it determines if it can be adopted by a new parent. At this time, the suitability of prospective new parents is determined by both the energy and ETX (link quality). First, the new parent of node j should satisfy (7) even after adopting node j. Second, to obtain a stable CTP topology, only a neighboring node satisfying the following ETX requirement can be selected as a new parent of node j:

$$ETX_{newParent} + linkETX_{(j,newParent)} < ETX_{originParent} + \min(linkETX_{(j,child)}), \tag{8}$$

where $ETX_{newParent}$ is the ETX of the new parent node, $linkETX_{(j,newParent)}$ is the linkETX between node j and its new parent, $ETX_{originParent}$ is the ETX of the original parent node, and $\min(linkETX_{(j,child)})$ is the minimum value of the linkETX between node j and its child nodes. Here, node j suppresses the loop occurrence by using the following three approaches:

1) Selecting only a neighboring node that satisfies (8) as its parent node: otherwise, its ETX may be greater than the ETX of its child nodes, which can cause a routing loop.
2) Excluding its child nodes from the parent candidate group: even though any of its child nodes satisfies (8), that node should not be the parent node because it also causes loop occurrence.
3) Preventing frequent changes of the parent node: it determines its parent only at the beginning of the time slot and keeps the parent unchanged during that time slot to prevent frequent changes of the parent node, which is likely to occur in the loop.

After receiving and analyzing positive reply messages from its child nodes, node i determines the most appropriate set of nodes that allow node i to satisfy (7) after they are adopted by their new parents. The number of nodes in this set can be one or more. Node i sends a change message to all the nodes in this set to detach them. Finally, by checking the value of

$E^{\text{alloc}}_{\text{remain}}(i, t+1)$, it decided whether to go to the normal mode or the control mode.

Algorithm 2 describes the pseudocode of the switch mode function, and Fig. 8 shows an example of the switch mode operation. In this example, node n_2 operates in switch mode (i.e., it does not have enough energy for next time slot) and broadcasts a switch message to its child nodes (line 1 of Algorithm 2). Node n_7 has a new parent candidate (node n_3), but node n_3 cannot satisfy (8). Therefore, node n_7 fails to find a new parent and sends back a negative reply to node n_2. However, node n_4 succeeds in finding a new parent (node n_1) because node n_1 satisfies (7) and (8) even after adopting node n_4. Therefore, node n_4 sends a positive reply message to node n_2 (line 4 of Algorithm 2). Node n_2 then recognizes that it can operate in normal mode by detaching node n_4 and hence sends a change message to node n_4 (from line 7 to 13 in Algorithm 2). Finally, node n_2 continues to operate in normal mode during the next time slot (line 14 of Algorithm 2).

Algorithm 2 Switch Mode Function

```
1:  BroadcastSwitchMessage(AllChildNodes of node_i);
2:  //Child nodes perform ReceiveSwitchMessage(),
    which invokes FindParentCandidate() and send the
    result;
3:
4:  ChangeNodesSet = FindChangeNodesSet();
5:  //Select child nodes that should change their parent;
6:
7:  while ∀(node_j ∈ ChangeNodesSet) do
8:      SendParentChangeMessage(node_j);
9:      //Node_j performs ReceiveParentChangeMessage(),
        which invokes SelectNewParent() and sends the
        result;
10:
11:     Recalculate E^alloc_remain(i, t+1);
12:
13: if E^alloc_remain(i, t+1) > 0 then
14:     ChangeMode(Normal);
15: else
16:     ChangeMode(Control);
17: return;
```

In terms of sensor energy consumption, computational overhead is negligible compared to data transmission overhead. Therefore, we analyze the overhead of Algorithm 2 performed by each node in terms of data transmission. Assuming m is the average number of node's child nodes and k is the average number of node's neighbors, the node in a switch mode sends a switch message to all child nodes as written in line 1 of Algorithm 2, so the complexity of $O(m)$ is necessary. Then, each child node that receives the switch message needs the complexity of $O(k-m)$ to find a new parent and thus requires the total complexity of $O(m(k-m))$ in line 1. Additionally, the loop starting from line 7 requires $O(m)$ complexity. Therefore, the overhead complexity of Algorithm 2 is $O(m(k-m))$. The complexity itself is low, but more importantly, this algorithm is executed once when the time slot starts, and the determined topology is not changed during the time slot. Therefore, it is expected that the amount of overhead described above is much less than the gain obtained through this algorithm.

F. CONTROL MODE OPERATION

If there is no appropriate set of child nodes for node i to detach to continue operating in normal mode, node i goes into the control mode to reduce data transmission. Note that even in this case, the child nodes that have given a positive reply message to node i should still be adopted by new parents to reduce the energy consumption of node i as much as possible even if it is not enough to allow node i to continue in normal mode.

In control mode, node i reduces the total amount of data transferred during a time slot to γ_i of the normal mode data transmission amount to avoid node blackout. γ_i, called the transmission control rate, can be expressed by

$$\gamma_i = \frac{S^{\max}_{\text{tx}}(i,t)}{S_{\text{all}}(i,t)}, \tag{9}$$

where $S_{\text{all}}(i,t)$ refers to the sum of the expected amount of data to be received from all the child nodes of node i and its own amount of sensing data during time slot t. Because we assume that the sensing rate of all nodes is constant, this value can be estimated from the number of descendant nodes node i has. $S^{\max}_{\text{tx}}(i,t)$ [43] is the maximum data size that node i can transmit during time slot t with the given energy and can be expressed by

$$S^{\max}_{\text{tx}}(i,t) = \frac{E_{\text{alloc}}(i,t) - E_{\text{sys}}(i,t)}{\beta d^{\alpha} linkETX_{(i,parent)}}. \tag{10}$$

Since the amount of data that can be transmitted in the control mode is limited, it is necessary to distinguish between data to be transmitted and data to be discarded. In solar-CTP, each node determines the data to transmit based on probability. In other words, by transmitting each of the received data with a probability of γ_i, $S^{\max}_{\text{tx}}(i,t)$ can be transmitted during this time slot.

Fig. 9 shows an example of the control mode operation. Fig. 9(a) shows the same situation as Fig. 8 except that node n_1 cannot meet (7) if it adopts node n_4 as a child node. In this case, node n_4 gives a negative reply message to node n_2, similar to node n_7. Therefore, node n_2 recognizes that there is no way to operate in normal mode. It hence enters the control mode and tries to prevent blackout by decreasing the total amount of transferred data, as shown in Fig. 9(b).

G. MOBILE SINK MOVEMENT

A mobile sink node moves to a random position at a specific period. This is very helpful in addressing the energy imbalance issue between the nodes located around the sink node and the outer nodes. The movement of the mobile sink

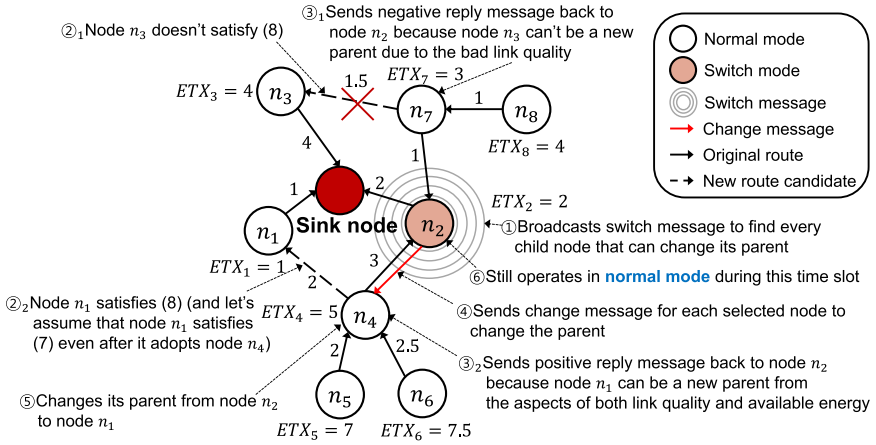

FIGURE 8. An example of switch mode operation.

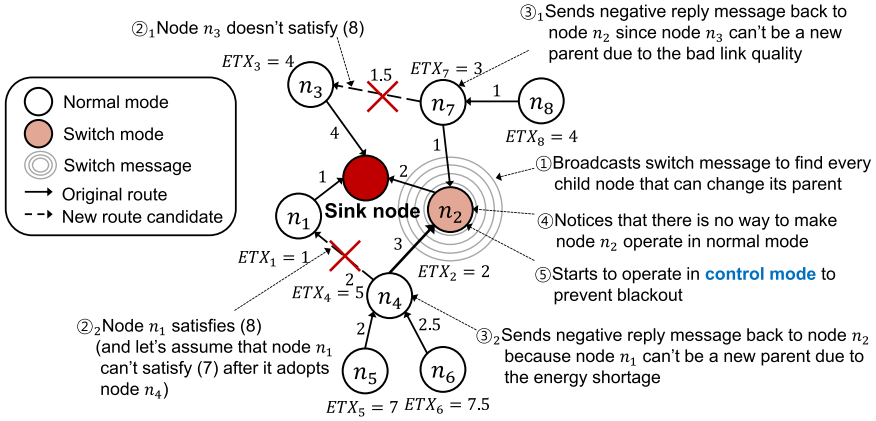

(a) An example of the process of falling into control mode

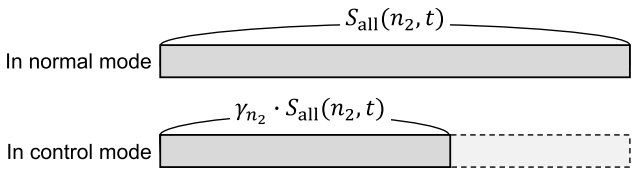

(b) Amount of data transferred during time slot t by node n_2

FIGURE 9. An example of control mode operation.

node can change the energy hotspot area to different places, as shown in Fig. 10.

The sink moves periodically and stays for a certain duration. After the sink completes its move, a beacon message is propagated eventually from the sink to all the nodes, and the CTP is reconfigured as shown in Fig. 10. That is, whenever a mobile sink moves at a specific period, the operations described in Section III-B through Section III-F are performed. Thus, the nodes that have consumed more energy before the sink node movement because of the close location to the sink will consume less energy after the sink has moved because they are now further away from the sink node in the new topology. This operation helps to eventually achieve energy balance over the network and reduces the blackout time of each node.

IV. PERFORMANCE EVALUATION

A. SIMULATION ENVIRONMENT

To evaluate the performance of the proposed scheme, we used SolarCastalia [44], which is a solar energy-harvesting WSN simulator. SolarCastalia provides the energy model of a solar-powered node, including the amount of energy harvested and consumed in various conditions measured from the specific solar-powered node [45].

We conducted simulations for 30 days and randomly deployed a total of 60, 80, and 100 sensor nodes over

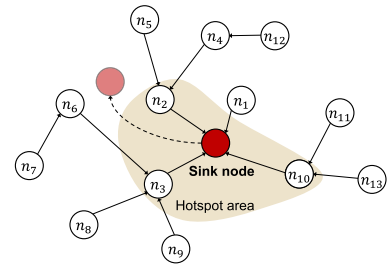

(a) Sink starts moving and all nodes remove information

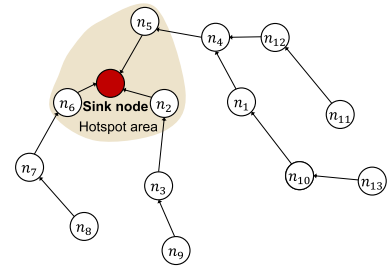

(b) CTP topology is reconfigured after sink has settled

FIGURE 10. CTP topology change due to mobile sink movement.

a 2500-m^2 field area. To evaluate the performance, we compared the proposed solar-CTP with ① the conventional CTP [6] considering the battery-based energy model denoted by the CTP and with ② ECTP-S and ③ BCTP-S, which are tailored by ECTP [39] and BCTP [36], respectively, for the solar energy-harvesting model with the balanced energy-allocation scheme [20]. Table 4 shows the detailed experimental environments.

TABLE 4. Simulation parameters.

Parameter	Value
Simulation time	30 days (720 rounds)
Number of nodes	60, 80, 100
Node topology	Random
Weather	Randomly selected
Field size	2500 m^2
Transmission range	10 m
Battery capacity	50 mAh
Sensing rate	40 bytes/min
α in (6)	4
β in (6)	0.9313 nJ/byte
Max. amount of energy harvested	64.22 J/day
Min. amount of energy harvested	25.68 J/day
Avg. amount of energy harvested	55.65 J/day
RX energy	0.1891 µJ/byte
Mobile sink moving location	Randomly selected
Mobile sink moving period	1 day

B. SIMULATION RESULTS

Fig. 11 shows the number of blackout nodes over time when 80 nodes were deployed. Most of the nodes suffered from blackout in the CTP because it does not incorporate an energy-harvesting model, resulting in a dramatic increase in blackout nodes with time. ECTP-S has a relatively small number of blackout nodes compared to the CTP, but blackout nodes still occur continuously. This shows that ECTP-S does not effectively utilize the harvested energy continuously. BCTP-S shows slightly fewer blackout nodes than ECTP-S. This is because loop occurrence is more frequent in ECTP-S, in which the ETX is simply increased when the energy is insufficient, whereas BCTP-S considers ETX when changing the parent node for energy balancing so that the loop occurrence is lower compared to that in ECTP-S. Last, the proposed scheme has the fewest blackout nodes among the various schemes at all times. This is because the proposed scheme selects an appropriate operation mode according to the energy status as well as the link condition even when a node has to communicate with many child nodes. In all schemes, the blackout nodes increase on days 9-11 and days 22-23 due to bad weather.

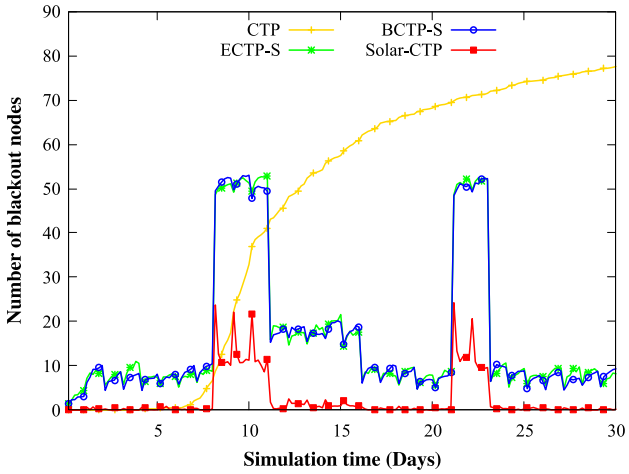

FIGURE 11. Number of blackout nodes (9th-11th day: rainy, 12th-16th day: cloudy, 22nd-23rd day: rainy, and others: sunny).

Fig. 12 shows the amount of data received at the sink node over time for 80 nodes. With the CTP, most of the nodes are unable to collect data after 15 days due to energy depletion.

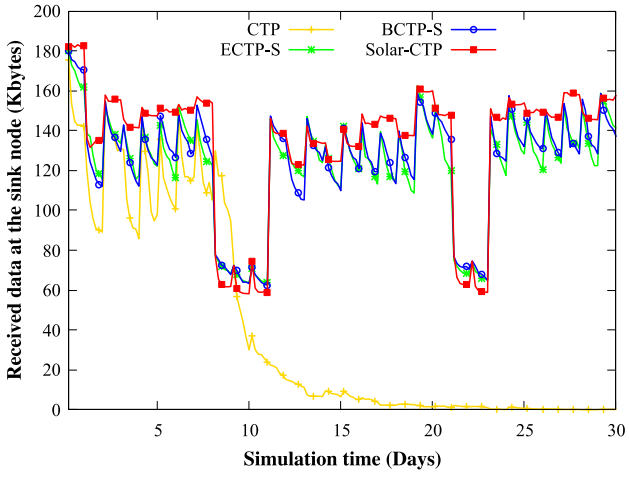

FIGURE 12. Amount of data received at the sink node (9th-11th day: rainy, 12th-16th day: cloudy, 22nd-23rd day: rainy, and others: sunny).

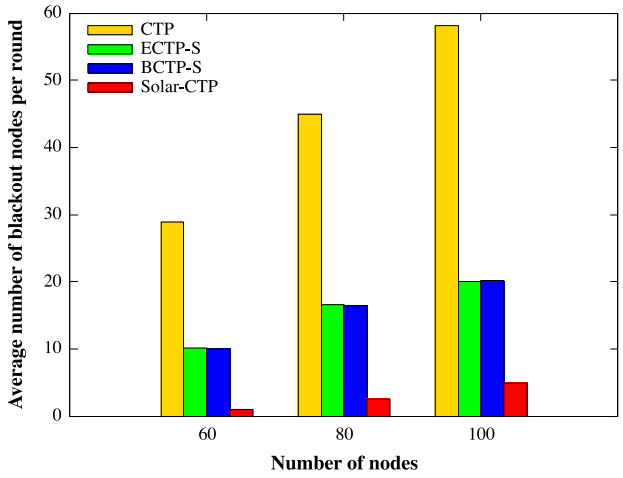

FIGURE 13. Average number of blackout nodes per round at various node counts.

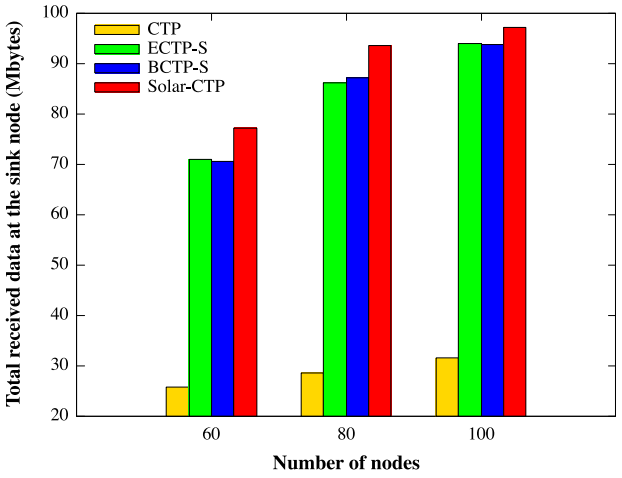

FIGURE 14. Total amount of received data at the sink node at various node counts.

On the other hand, solar-CTP generally showed better results than ECTP-S and BCTP-S; only when the weather was severe did solar-CTP show similar results to these two schemes. The interpretation of these results is very important. Although the total amount of data with solar-CTP is similar to that with ECTP-S and BCTP-S in bad weather, the number of active nodes in solar-CTP is much greater than that in the others. Considering that the utility of a WSN is measured not only by the total amount of data collected but also by the spatial coverage, these results indicate that solar-CTP successfully maximized the coverage and hence the utility of the network by adjusting the transmission control rate γ according to energy availability.

Fig. 13 shows the number of blackout nodes according to the number of nodes deployed. The proposed scheme has the fewest blackout nodes regardless of the number of nodes. This shows the scalability of solar-CTP. Because solar-CTP operates in a completely distributed manner, it exhibits good performance regardless of the number of nodes. The figure shows that most of the nodes were blacked out for the CTP, and ECTP-S and BCTP-S also had more blackout nodes than solar-CTP. This is because the relay nodes had to receive more data as the number of nodes increased. Accordingly, many relay nodes, including the nodes around the sink, suffered from blackout.

Fig. 14 shows the total amount of data received at the sink node according to the number of nodes deployed. The proposed scheme collected more data than the other schemes. The amount of data received is affected by the number of blackout nodes as described above. Additionally, for ECTP-S and BCTP-S, the blackout of the nodes around the sink had a particularly significant impact on the amount of data received. Finally, as explained previously, it is important to note that higher quality data were received with our solar-CTP scheme compared to the other schemes because the data sources were more diverse in the network.

Fig. 15 shows the number of blackout nodes at various link qualities for 80 nodes. ECTP-S and BCTP-S showed fewer

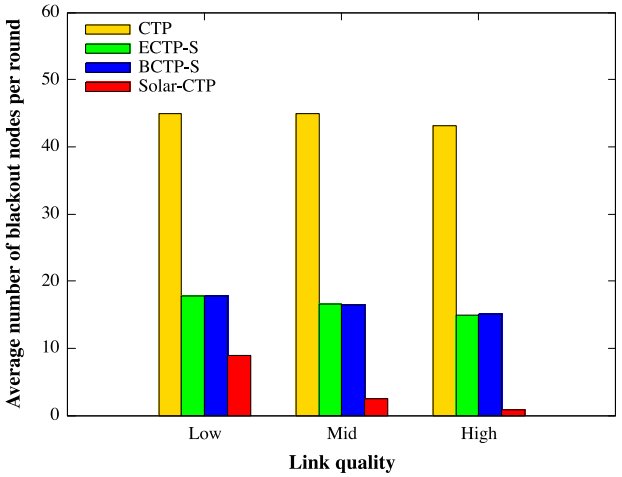

FIGURE 15. Average number of blackout nodes per round at various link qualities.

blackout nodes as the link quality improved. In an environment where the link quality is poor, many communication attempts are required for the successful transmission of even a single packet. Accordingly, nodes frequently switch their parent nodes to find better paths. This results in a large number of blackout nodes because of loop occurrence and blackout at the nodes near the sink node. However, the proposed scheme takes the energy into account when selecting a parent node, resulting in fewer blackout nodes than the other schemes regardless of the link quality.

Fig. 16 shows the total amount of data received at the sink node for the four schemes according to the link qualities for 80 nodes. For ECTP-S and BCTP-S, in agreement with the previous experimental results, the data from the nodes did not reach the sink node because of the routing loops caused by frequent parent changes and retransmission in environments with poor link quality. On the other hand, the proposed scheme collected more data than the other schemes regardless of the link quality by considering both the energy and ETX simultaneously for changing the parent. Again, note that the

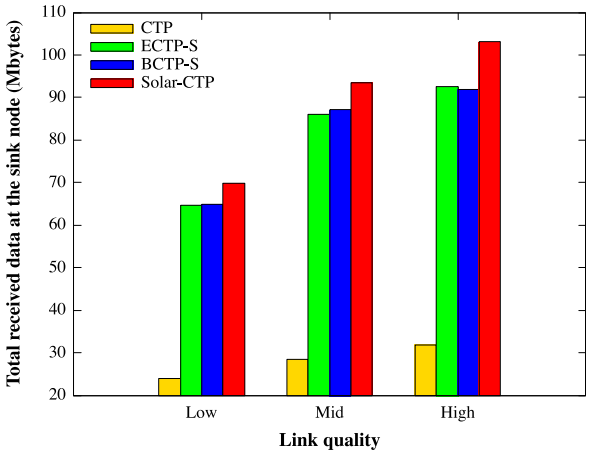

FIGURE 16. Total amount of received data at the sink node at various link qualities.

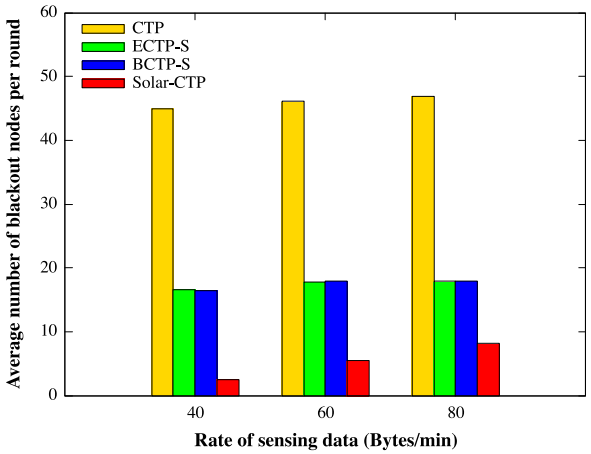

FIGURE 17. Average number of blackout nodes per round at various rates of sensing data.

quality of data received with our solar-CTP was superior compared to the other schemes, as explained previously.

Figs. 17 and 18 show the number of blackout nodes and amount of data received at the sink node according to the data sensing rates for 80 nodes. The CTP shows the highest number of blackout nodes and the smallest amount of data collected for all sensing rates. ECTP-S and BCTP-S show similar results and have much higher numbers of blackout nodes and smaller amounts of data collected than the proposed scheme. The proposed scheme collected the largest amount of data among all the schemes owing to the topology configuration that considered both link quality and energy status. However, for ECTP-S, BCTP-S, and the proposed scheme, the amount of data received at the sink node was reduced when the sensing data rate was 80 bytes/min. This is because of the loss of a large amount of data due to the increase in the blackout frequency of the relay nodes.

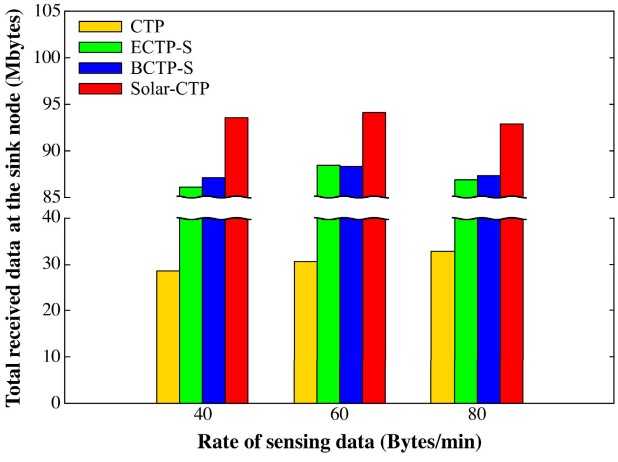

FIGURE 18. Total amount of received data at the sink node at various rates of sensing data.

V. CONCLUSIONS

The conventional CTP scheme can perform efficient routing based on the link quality; furthermore, it has the advantage of a fair data transfer rate. However, it has some drawbacks, such as loop occurrence due to blackout nodes and vulnerability to energy imbalance between nodes at different levels in the CTP tree topology. In this paper, we proposed solar-CTP, which is appropriate for WSNs consisting of solar energy-harvesting wireless sensor nodes with a mobile sink node. The proposed scheme reduced the occurrence of blackout nodes by 50%–98%, increased the amount of data collected at the sink node by up to 4%–227%, and improved the quality of the data received compared to the other CTP-based variants.

In the future research, we intend to develop solar-CTP suitable for mobile sinks that have non-fixed moving cycle or move continuously. We will also study solar-CTP for mobile WSN where sensor nodes move.

REFERENCES

[1] J. Yick, B. Mukherjee, and D. Ghosal, "Wireless sensor network survey," *Comput. Netw.*, vol. 52, no. 12, pp. 2292–2330, Aug. 2008.

[2] I. F. Akyildiz, W. Su, Y. Sankarasubramaniam, and E. Cayirci, "Wireless sensor networks: A survey," *Comput. Netw.*, vol. 38, no. 4, pp. 393–422, 2002.

[3] S. Sudevalayam and P. Kulkarni, "Energy harvesting sensor nodes: Survey and implications," *IEEE Commun. Surveys Tuts.*, vol. 13, no. 3, pp. 443–461, 3rd Quart., 2011.

[4] X. Wu, G. Chen, and S. K. Das, "On the energy hole problem of nonuniform node distribution in wireless sensor networks," in *Proc. IEEE Int. Conf. Mobile Ad Hoc Sensor Syst. (MASS)*, Oct. 2006, pp. 180–187.

[5] C. Tunca, S. Isik, M. Y. Donmez, and C. Ersoy, "Distributed mobile sink routing for wireless sensor networks: A survey," *IEEE Commun. Surveys Tuts.*, vol. 16, no. 2, pp. 877–897, 2nd Quart., 2014.

[6] O. Gnawali, R. Fonseca, K. Jamieson, M. Kazandjieva, D. Moss, and P. Levis, "CTP: An efficient, robust, and reliable collection tree protocol for wireless sensor networks," *ACM Trans. Sensor Netw.*, vol. 10, no. 1, pp. 1–49, Nov. 2013.

[7] D. S. J. De Couto, D. Aguayo, J. Bicket, and R. Morris, "A high-throughput path metric for multi-hop wireless routing," in *Proc. 9th Annu. Int. Conf. Mobile Comput. Netw. (MobiCom)*, 2003, pp. 134–146, doi: 10.1145/938985.939000.

[8] A. Kansal, J. Hsu, S. Zahedi, and M. B. Srivastava, "Power management in energy harvesting sensor networks," *ACM Trans. Embedded Comput. Syst.*, vol. 6, no. 4, p. 32, Sep. 2007.

[9] J. A. Khan, H. K. Qureshi, and A. Iqbal, "Energy management in wireless sensor networks: A survey," *Comput. Elect. Eng.*, vol. 41, pp. 159–176, Jan. 2015.

[10] A. Wang, W. B. Heinzelman, A. Sinha, and A. P. Chandrakasan, "Energy-scalable protocols for battery-operated microsensor networks," *J. VLSI Signal Process. Syst. Signal Image Video Technol.*, vol. 29, no. 3, pp. 223–237, 2001.
[11] C. Park, K. Lahiri, and A. Raghunathan, "Battery discharge characteristics of wireless sensor nodes: An experimental analysis," in *Proc. 2nd Annu. IEEE Commun. Soc. Conf. Sensor Ad Hoc Commun. Netw. (SECON)*, 2005, pp. 430–440.
[12] C. Ma and Y. Yang, "Battery-aware routing for streaming data transmissions in wireless sensor networks," *Mobile Netw. Appl.*, vol. 11, no. 5, pp. 757–767, Oct. 2006.
[13] Y. Cho, Y. Kim, and N. Chang, "PVS: Passive voltage scaling for wireless sensor networks," in *Proc. Int. Symp. Low Power Electron. Design (ISLPED)*, 2007, pp. 135–140, doi: 10.1145/1283780.1283810.
[14] H. Long, Y. Liu, Y. Wang, R. P. Dick, and H. Yang, "Battery allocation for wireless sensor network lifetime maximization under cost constraints," in *Proc. Int. Conf. Comput.-Aided Design (ICCAD)*, 2009, pp. 705–712.
[15] K. S. Adu-Manu, N. Adam, C. Tapparello, H. Ayatollahi, and W. Heinzelman, "Energy-harvesting wireless sensor networks (EH-WSNs): A review," *ACM Trans. Sensor Netw.*, vol. 14, no. 2, pp. 10:1–10:50, 2018.
[16] A. Kansal, D. Potter, and M. B. Srivastava, "Performance aware tasking for environmentally powered sensor networks," *SIGMETRICS Perform. Eval. Rev.*, vol. 32, no. 1, pp. 223–234, 2004, doi: 10.1145/1012888.1005714.
[17] C. Moser, L. Thiele, D. Brunelli, and L. Benini, "Adaptive power management in energy harvesting systems," in *Proc. Design, Autom. Test Eur. Conf. Exhib. (DATE)*, Apr. 2007, pp. 1–6.
[18] J. R. Piorno, C. Bergonzini, D. Atienza, and T. S. Rosing, "Prediction and management in energy harvested wireless sensor nodes," in *Proc. 1st Int. Conf. Wireless Commun., Veh. Technol., Inf. Theory Aerosp. Electron. Syst. Technol. (Wireless VITAE)*, May 2009, pp. 6–10.
[19] A. Cammarano, C. Petrioli, and D. Spenza, "Pro-energy: A novel energy prediction model for solar and wind energy-harvesting wireless sensor networks," in *Proc. IEEE 9th Int. Conf. Mobile Ad-Hoc Sensor Syst. (MASS)*, Oct. 2012, pp. 75–83.
[20] D. K. Noh and K. Kang, "Balanced energy allocation scheme for a solar-powered sensor system and its effects on network-wide performance," *J. Comput. Syst. Sci.*, vol. 77, no. 5, pp. 917–932, Sep. 2011. [Online]. Available: http://www.sciencedirect.com/science/article/pii/S0022000010001236
[21] Y. Zhang, S. He, and J. Chen, "Data gathering optimization by dynamic sensing and routing in rechargeable sensor networks," *IEEE/ACM Trans. Netw.*, vol. 24, no. 3, pp. 1632–1646, Jun. 2016.
[22] Y. Yang, L. Wang, D. K. Noh, H. K. Le, and T. F. Abdelzaher, "SolarStore: Enhancing data reliability in solar-powered storage-centric sensor networks," in *Proc. 7th Int. Conf. Mobile Syst., Appl., Services (Mobisys)*, 2009, pp. 333–346.
[23] M. Kang, I. Yoon, and D. Noh, "Efficient location service for a mobile sink in solar-powered wireless sensor networks," *Sensors*, vol. 19, no. 2, p. 272, Jan. 2019.
[24] S. Herrería-Alonso, A. Suárez-González, M. Rodríguez-Pérez, R. F. Rodríguez-Rubio, and C. López-García, "A solar altitude angle model for efficient solar energy predictions," *Sensors*, vol. 20, no. 5, p. 1391, Mar. 2020.
[25] C. Wang, J. Li, Y. Yang, and F. Ye, "Combining solar energy harvesting with wireless charging for hybrid wireless sensor networks," *IEEE Trans. Mobile Comput.*, vol. 17, no. 3, pp. 560–576, Mar. 2018.
[26] M. Angurala, M. Bala, and S. S. Bamber, "Performance analysis of modified AODV routing protocol with lifetime extension of wireless sensor networks," *IEEE Access*, vol. 8, pp. 10606–10613, 2020.
[27] N. Baccour, A. Koubâa, L. Mottola, M. A. Zúñiga, H. Youssef, C. A. Boano, and M. Alves, "Radio link quality estimation in wireless sensor networks: A survey," *ACM Trans. Sensor Netw.*, vol. 8, no. 4, pp. 1–33, Sep. 2012.
[28] C. E. Perkins and P. Bhagwat, "Highly dynamic destination-sequenced distance-vector routing (DSDV) for mobile computers," *ACM SIGCOMM Comput. Commun. Rev.*, vol. 24, no. 4, pp. 234–244, Oct. 1994.
[29] C. Gomez, P. Salvatella, O. Alonso, and J. Paradells, "Adapting AODV for IEEE 802.15.4 mesh sensor networks: Theoretical discussion and performance evaluation in a real environment," in *Proc. Int. Symp. a World Wireless, Mobile Multimedia Networks(WoWMoM)*, 2006, pp. 159–170.
[30] TinyOS. (2009). *The MultiHopLQI Protocol*. [Online]. Available: https://github.com/tinyos/tinyos-main/tree/master/tos/lib/net/lqi
[31] T. Winter, P. Thubert, A. Brandt, J. W. Hui, R. Kelsey, P. Levis, K. Pister, R. Struik, J.-P. Vasseur, and R. K. Alexander, *RPL: IPv6 Routing Protocol for Low-Power and Lossy Networks*, document RFC 6550, 2012, pp. 1–157.
[32] P. Levis, S. Madden, J. Polastre, R. Szewczyk, K. Whitehouse, A. Woo, D. Gay, J. Hill, M. Welsh, E. Brewer, and D. Culler, "TinyOS: An operating system for sensor networks," in *Ambient Intelligence*. Berlin, Germany: Springer, 2005, pp. 115–148.
[33] U. Colesanti and S. Santini, "The collection tree protocol for the castalia wireless sensor networks simulator," Dept. Comput. Sci., ETH Zürich, Zürich, Switzerland, Tech. Rep. 729, 2011, vol. 729.
[34] R. Fonseca, O. Gnawali, K. Jamieson, and P. Levis, "Four-bit wireless link estimation," in *Proc. ACM Hot Topics Netw. (HotNets)*, 2007, pp. 1–7.
[35] P. Levis, N. Patel, D. Culler, and S. Shenker, "Trickle: A self-regulating algorithm for code propagation and maintenance in wireless sensor networks," in *Proc. USENIX Symp. Netw. Syst. Design Implement. (NSDI)*, 2004, pp. 15–28.
[36] J. Zhao, L. Wang, W. Yue, Z. Qin, and M. Zhu, "Load migrating for the hot spots in wireless sensor networks using CTP," in *Proc. IEEE Int. Conf. Mobile Ad-Hoc Sensor Netw. (MSN)*, Dec. 2011, pp. 167–173.
[37] J. Flathagen, E. Larsen, P. E. Engelstad, and O. Kure, "O-CTP: Hybrid opportunistic collection tree protocol for wireless sensor networks," in *Proc. IEEE Int. Workshop Practical Issues Building Sensor Netw. Appl. (SenseApp)*, Oct. 2012, pp. 943–951.
[38] F. Entezami, M. Tunicliffe, and C. Politis, "RCTP: An enhanced routing protocol based on collection tree protocol," *Int. J. Distrib. Sensor Netw.*, vol. 11, no. 4, Apr. 2015, Art. no. 363107.
[39] J. Zhang, Z. Yang, B. Wang, H. Sun, and X. Sun, "E-CTP: An energy-balanced collection tree protocol for power constrained wireless sensor networks," *Int. J. Grid Distrib. Comput.*, vol. 7, no. 2, pp. 115–126, Apr. 2014.
[40] G. Sun, X. Shang, and Y. Zuo, "La-CTP: Loop-aware routing for energy-harvesting wireless sensor networks," *Sensors*, vol. 18, no. 2, p. 434, Feb. 2018.
[41] D. Krynicki and R. Liscano, "An analysis of the directional preference ETX measure for the collection tree protocol in mobile sensor networks," *Procedia Comput. Sci.*, vol. 155, pp. 351–359, 2019.
[42] T. Melodia, D. Pompili, and I. F. Akyildiz, "Optimal local topology knowledge for energy efficient geographical routing in sensor networks," in *Proc. IEEE Int. Conf. Comput. Commun. (INFOCOM)*, vol. 3, Mar. 2004, pp. 1705–1716.
[43] I. Yoon and D. Noh, "Energy-aware control of data compression and sensing rate for wireless rechargeable sensor networks," *Sensors*, vol. 18, no. 8, p. 2609, Aug. 2018.
[44] J. M. Yi, M. J. Kang, and D. K. Noh, "SolarCastalia: Solar energy harvesting wireless sensor network simulator," *Int. J. Distrib. Sensor Netw.*, vol. 11, no. 6, Jun. 2015, Art. no. 415174.
[45] *Ez430-rf2500 Development Tool User's Guide*, document SLAU227E, Texas Instruments, 2009.

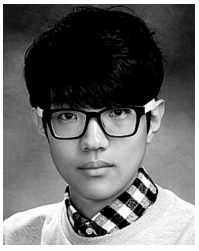

SEOK HYUN CHEONG received the B.S. degree in smart systems software from Soongsil University, South Korea, in 2019, where he is currently pursuing the M.S. degree with the Department of Software Convergence. His research interests include wireless sensor networks, cyber physical systems, embedded system software, and ubiquitous sensor networks.

MINJAE KANG received the B.S. degree in computer engineering from Paichai University, in 2011, and the combined M.S.-Ph.D. degree in electronic engineering from Soongsil University, in 2019. He is currently a Postdoctoral Researcher with Soongsil University. His research interests include embedded systems, cyber physical systems, and ubiquitous sensor networks.

YOUNGHYUN KIM (Member, IEEE) received the B.S. degree (Hons.) in computer science and engineering and the Ph.D. degree in electrical engineering and computer science from Seoul National University, Seoul, South Korea, in 2007 and 2013, respectively. From 2013 to 2016, he was a Postdoctoral Research Assistant with the School of Electrical and Computer Engineering, Purdue University, West Lafayette, IN, USA. He is currently an Assistant Professor and a Grainger Institute for Engineering Faculty Scholar with the Department of Electrical and Computer Engineering, University of Wisconsin–Madison, Madison, WI, USA. His current research interests include energy-efficient computing, cyber-physical systems security, and the Internet of Things.

MINHO PARK (Member, IEEE) received the B.S. and M.S. degrees in electronics engineering from Korea University, in 2000 and 2002, respectively, and the Ph.D. degree from the School of Electrical Engineering and Computer Science, Seoul National University, Seoul, South Korea, in 2010. He is currently an Associate Professor with the School of Electronic Engineering, Soongsil University, Seoul. His current research interests include wireless networks, vehicular communication networks, network security, and cloud computing.

JINHO PARK received the B.S. and M.S. degrees in applied mathematics, in 1999 and 2001, respectively, and the Ph.D. degree in computer science from the Korea Advanced Institute of Science and Technology, in 2007. He is currently an Associate Professor with the Global School of Media, Soongsil University, South Korea. His research interests include augmented reality and machine learning.

DONG KUN NOH (Member, IEEE) received the B.S., M.S., and Ph.D. degrees in computer science and engineering from Seoul National University, in 2000, 2002, and 2007, respectively. From 2007 to 2010, he was a Postdoctoral Researcher with the University of Illinois at Urbana-Champaign. From 2017 to 2018, he was a Visiting Scholar with the University of Wisconsin–Madison. He is currently an Associate Professor with the Department of Software Convergence, Soongsil University. His research interests include embedded systems, mobile computing, and ubiquitous sensor networks.